7-1-2008

Probing the functional tolerance of the b subunit of Escherichia coli ATP synthase for sequence manipulation through a chimera approach.

Yumin Bi

Joel C Watts

Pamela Krauss Bamford

Lee-Ann K Briere

Stanley D Dunn

Follow this and additional works at: https://ir.lib.uwo.ca/biochempub

Part of the Biochemistry Commons

Probing the functional tolerance of the *b* subunit of *Escherichia coli* ATP synthase for sequence manipulation through a chimera approach[§]

Yumin Bi, Joel C. Watts[1], Pamela Krauss Bamford[2], Lee-Ann K. Briere and Stanley D. Dunn*

Department of Biochemistry, University of Western Ontario, London, Ontario N6A 5C1 Canada

*Corresponding author. Tel: +1 519 661 3055; fax: +1 519 661 3175. E-mail: sdunn@uwo.ca
[1]Present address: Centre for Research in Neurodegenerative Diseases, University of Toronto, Toronto, Ontario, Canada M5S 3H2
[2]Present address: Research In Motion Limited, Waterloo, Ontario, Canada N2L 3L3

Key words: ATP synthase, *b* subunit, chimeric protein, coiled coil, right-handed coiled coil, hendecad pattern

Abbreviations: ACMA, 9-amino-6-chloro-2-methoxyacridine; Ag84, antigen-84; CD, circular dichroism; DSC, differential scanning calorimetry; FCCP, carbonyl cyanide *p*-(trifluoromethoxy)phenylhydrazone; VATE, E subunit of V-ATPase.

Summary

          A dimer of 156-residue *b* subunits forms the peripheral stator stalk of eubacterial ATP synthase. Dimerization is mediated by a sequence with an unusual 11-residue (hendecad) repeat pattern, implying a right-handed coiled coil structure. We investigated the potential for producing functional chimeras in the *b* subunit of *Escherichia coli* ATP synthase by replacing parts of its sequence with corresponding regions of the *b* subunits from other eubacteria, sequences from other polypeptides having similar hendecad patterns, and sequences forming left-handed coiled coils. Replacement of positions 55-110 with corresponding sequences from *Bacillus subtilis* and *Thermotoga maritima b* subunits resulted in fully functional chimeras, judged by support of growth on nonfermentable carbon sources. Extension of the *T. maritima* sequence N-terminally to position 37 or C-terminally to position 124 resulted in slower but significant growth, indicating retention of some capacity for oxidative phosphorylation. Portions of the dimerization domain between 55 and 95 could be functionally replaced by segments from two other proteins having a hendecad pattern, the distantly related E subunit of the *Chlamydia pneumoniae* V-type ATPase and the unrelated Ag84 protein of *Mycobacterium tuberculosis*. Extension of such sequences to position 110 resulted in loss of function. None of the chimeras that incorporated the leucine zipper of yeast GCN4, or other left-handed coiled coils, supported oxidative phosphorylation, but substantial ATP-dependent proton pumping was observed in membrane vesicles prepared from cells expressing such chimeras. Characterization of chimeric soluble *b* polypeptides *in vitro* showed their retention of a predominantly helical structure. The *T. maritima b* subunit chimera melted cooperatively with a midpoint more than 20 °C higher than the normal *E. coli* sequence. The GCN4 construct melted at a similarly high temperature, but with much reduced cooperativity, suggesting a degree of structural disruption. These studies provide insight into the structural and sequential requirements for stator stalk function.

1. Introduction

Ion-translating ATP synthase/ATPases of the F-, A-, or V-ATPase types utilize a rotational mechanism for coupling ion movement through the membrane-bound sector, F_0, A_0, or V_0, to the synthesis or hydrolysis of ATP by the peripheral catalytic sector, F_1, A_1, or V_1. In the prototypical F-ATP synthase of *Escherichia coli*, the central rotor subcomplex is composed the $\gamma\varepsilon c_{10}$ while the stator is composed of $\alpha_3\beta_3\delta ab_2$. The *b* subunit dimer forms the peripheral stator stalk, linking the *a* subunit of F_0 with $\alpha_3\beta_3\delta$ of F_1. The stator stalk must resist the torque imposed by the rotor so that the γ subunit turns inside $\alpha_3\beta_3$, generating conformational changes associated with ATP synthesis. The ATP synthases of most eubacteria have homodimeric stator stalks, but photosynthetic species, amongst others, contain heterodimers of two *b*-type subunits, *b* and *b'*. The stator stalks of chloroplast ATP synthase are also heterodimeric, with subunits denoted I and II. The stator stalk of mitochondrial ATP synthase has a different architecture; one of its subunits is called *b* but bears little sequence similarity to the eubacterial and chloroplast *b* family. See recent reviews of ATP synthase [1-4].

The soluble domain of *E. coli b*, expressed without the N-terminal transmembrane domain, has been characterized as a highly extended, helical dimer with substantial coiled coil character [5-8]. Deletion analysis identified a central dimerization domain bounded approximately by positions 53 and 122[8]. The C-terminal region is essential for binding $\alpha_3\beta_3\delta$ [9, 10], and may be called the δ-binding or F_1-binding domain, while the region between the membrane and the dimerization domains has been termed the tether domain [11].

The sequence of eubacterial *b* is not well conserved, but multiple sequence alignments reveal an unusual 11-residue (hendecad) pattern in the dimerization domain [11-13]. Hendecad patterns are thought to be typical of right-handed coiled coils [14, 15]. Hendecad positions are denoted ***a*** through ***k***; the ***a*** and ***h*** positions in the *b* family are most often occupied by small residues, usually alanine, while the ***d*** and ***e*** positions are often occupied by larger nonpolar residues. These positions form a hydrophobic, right-handed strip on the helix b_{61-122} crystal structure [12]. Protein chemical evidence has shown this strip to be the dimerization interface, so it seems likely that dimerization will form a novel two-stranded, right-handed coiled coil [13]. However, modeling studies and analysis of inter-residue distances by ESR have led to the proposal that a left-handed coiled coil is also possible [16, 17], so the nature of the structure remains controversial.

In the current work, we sought to ask what modifications to the sequence of *b* will support its function as the stator stalk. Since few point mutations of *b* affect function [18, 19], we adopted the approach of constructing chimeras in which substantial sections of the *E. coli b* polypeptide are replaced by exogenous sequences. We began by substituting corresponding regions from other eubacterial *b* subunits, then extended the approach to sequences from other proteins with hendecad repeats that should be compatible with RHCC, and finally to left-handed

coiled coils.   The effects of these substitutions provide insight into the parts of *b* that tolerate changes, and the types of change they tolerate without loss of function.

2. Materials and methods

2.1 Materials

Genomic DNA from *Thermotoga maritima* was purchased from the American Type Culture Collection. Genomic DNA from *Chlamydia pneumoniae* AR3 was a kind gift from Dr. Robert Brunham of the University of British Columbia Centre for Disease Control, Vancouver British Columbia, Canada. Plasmid pPH5253 [20] carrying the gene encoding Ag84 from *Mycobacterium tuberculosis* was kindly provided by Dr. Peter W. Hermans, Laboratory of Pediatric Infectious Diseases, Radboud University Nijmegen Medical Centre, Nijmegen, The Netherlands. *Saccharomyces cereviseae* DNA was kindly provided by Dr. Chris Brandl, Department of Biochemistry, University of Western Ontario. *Bacillus subtilis* DNA was prepared from bacterial cells. *E. coli* strain KM2 [21], carrying a chromosomal deletion of *uncF*, pDM8 [6], carrying a synthetic *uncF* gene, and pBAD24 [22], an expression vector utilizing the arabinose control system, have been described.

Synthetic oligonucleotides were obtained from Sigma. Monoclonal antibody α-II was the generous gift of Drs. Rod Capaldi and Robert Aggeler of the University of Oregon, Eugene, Oregon. Polyclonal antibodies to the soluble domain of *E. coli b* subunit were raised in a rabbit and purified by affinity chromatography on a column of b_{MERC} coupled to Sulfo-link resin (Pierce), prepared as described [9].

2.2 Plasmid construction

Recombinant DNA procedures were carried out by standard methods. To construct pJW3, the entire *uncF* gene (encoding *b*) of *T. maritima* was amplified by PCR using 5'-CGGCGGTACCATAGAGGCATTGTGCTGTGGGCTTTCTGGAG-3' as forward primer and 5'-GACGGCAGCTTGAGACCTTATGACTTTTCTATCTCCT-3' as reverse primer. The forward primer contains a synthetic KpnI site, a Shine-Dalgarno sequence, and changes the start codon from TTG to GTG, in order to match *E. coli b*. The reverse primer contains a BsaI site that leaves a 5' overhang compatible with HindIII; this strategy was used since *T. maritima uncF* contains an internal HindIII site. The PCR product was cut with KpnI and BsaI and then ligated into the corresponding KpnI and HindIII sites in pDM8 in order to make pJW3. Sequences encoding natural or chimeric *b* subunits were transferred from pDM8-type plasmids, with the lac gene expression control system into pBAD24 [22] with the arabinose gene expression control system using the EcoRI and HindIII sites. The plasmid carrying the synthetic *b* sequence in pBAD24 was called pSD205.

For chimera construction, primers included restriction enzyme sites suitable for cloning products in-frame into the synthetic *uncF* sequence in pDM8 or pSD205. DNA for preparing chimeras incorporating sequences from *b* subunits of *T. maritima* or *B. subtilis*, the E subunit of the V-ATPase of *C. pneumoniae*, the Ag84 protein of *M. tuberculosis* Ag84, or yeast GCN4, were obtained by PCR amplification from either genomic DNA or plasmids containing the

appropriate cloned gene.   DNA for preparing chimeras incorporating sequences from rabbit tropomyosin or human Eea1 was prepared synthetically by primed synthesis from the overlapping 3' ends. Specific information regarding the regions of exogenous amino acid residues incorporated into b and the regions of the *E. coli b* sequence that were replaced may be found in Tables 1 and 2. For chimeric fusions beginning at particular residues of the *E. coli b* sequence, the following restriction sites in pDM8 or pSD205 were used: Gln-37, MfeI; Asp-55, Lys-58, Ala-61, or Thr-62, BglII; Lys-67 or Ala-68, AflII; Glu-71, Ala 72, Gln-73, or Arg-83, StyI.   For chimeric fusions ending at particular residues of the *E. coli b* sequence, the following restriction sites in pDM8 or pSD205 were used: Asn-80, AlwNI; Lys-91, Glu-95, or Val-102, BsiWI; Glu-108, Glu-110, BlpI; Val-124, SfiI. All sequences derived by PCR were confirmed by DNA sequencing.

Plasmids encoding soluble forms of the Tm-1, GCN4-1, and Ag84-1 chimeras in the context of b_{34-156} [6] were constructed by transferring the 176-bp BglII-BlpI fragments from pSD200, pSD203 and pSD204 respectively, into pSD114, replacing the synthetic sequence encoding those portions of *E. coli b*, to produce plasmids pSD207, pSD208, and pSD209.

2.3 Minimal media growth tests and characterization of membrane activities

M9 minimal media plates were prepared as previously described [23] containing either glucose, succinate, or acetate as the sole carbon source. Either IPTG or arabinose was added to final concentrations of 0, 1, 3, 10, and 30 µM. The appropriate plasmids were transformed into *E. coli* strain KM2 ($\Delta uncF$) and were grown to an A_{600} of approximately 0.1 in L broth. Cells were spun down and the cell pellets were washed with 0.9% NaCl. Following resuspension in fresh 0.9% NaCl, cells were streaked out. Plates were incubated at 37 °C and growth was evaluated using a dissecting microscope and a grid for measuring colony size.

Membrane vesicles for assessment of ATPase and ATP-dependent proton pumping were prepared from cells of strain KM2, carrying the appropriate plasmids, grown on rich media in the presence of levels of inducers that had been shown to lead to synthesis of normal levels of b subunit from the control *E. coli* gene, pDM8 for the lac system or pSD205 for the arabinose system.   In particular, cells carrying pDM8 and derivatives were grown with vigorous shaking at 37 °C in L broth containing 10 mM sodium phosphate, pH 7.0, 15 µM IPTG, and ampicillen at 40 µg/ml and harvested when A_{600} reached 0.8. Cells carrying pSD205 and derivatives were grown similarly but in L broth containing 10 mM sodium phosphate, pH 7.0, 100 µM arabinose, 0.4% glycerol, and ampicillen at 40 µg/ml and harvested when A600 reached 1.0. For preparation of membranes, cells were resuspended in 50 mM sodium phosphate, pH7.5, 5 mM MgCl₂, containing 10% glycerol and broken by passage through a French pressure cell at 20,000 psi. Following sedimentation of large debris by centrifugation in a JA-20 rotor at 10,000 rpm for 10 min, the membrane fraction was collected by sedimentation in a Ti-50 rotor at 38,000 rpm for 90 min. The pellet was washed by suspension in 10 mM Mops-NaOH, pH 7.5, containing 250 mM sucrose, 5 mM MgCl₂, 10% methanol, and sedimented as before. The final pellet was resuspended in a small volume of the same buffer and stored at –80 °C.

Membrane ATPase content was determined as described previously [24], using the "released ATPase" assay conditions. ATP-dependent proton pumping was measured by the quenching of 9-amino-6-chloro-2-methoxyacridine (ACMA) as described [24].

2.4 Purification of proteins.

E. coli b_{34-156} was expressed from plasmid pSD114 and purified as described [6]. Purification was followed by SDS-PAGE. Chimeric forms of b_{34-156} carrying the Tm-1, GCN4-1, and Ag84-1 sequences were expressed from plasmids pSD207, pSD208 and pSD209, respectively. Expression, extraction, and precipitation with 45% saturated ammonium sulfate followed the protocol for b_{34-156}.

For purification of b_{34-156}Tm-1, the redissolved and dialyzed pellet was applied to a column of DEAE-Sepharose in 50 mM Tris-HCl, pH 8.0, 1 mM EDTA, and eluted with a linear gradient of NaCl in the same buffer. Peak fractions were subjected to a second step of ion exchange chromatography at pH 8 on a High Performance Q-Sepharose column. Peak fractions were precipitated with ammonium sulfate, redissolved in buffer and given a final step of size-exclusion chromatography on a column of Sephacryl S-200.

For purification of both b_{34-156}GCN4-1 and b_{34-156}Ag84-1, the redissolved and dialyzed pellets was applied to a column of Fast-Flow Q-Sepharose at pH 8.0 and eluted with a gradient of NaCl. Following dialysis, the peak fractions were applied to a High Performance Q-Sepharose column in 25 mM imidazole-HCl buffer at pH 6.4 and eluted with a salt gradient. This step was then repeated at pH 8.0 in Tris-HCl buffer to obtain pure proteins. In all cases, preparations with a high state of purity appropriate for biophysical analyses were obtained. Protein concentrations were measured by the Coomassie blue binding assay [25] and corrected by a factor of 0.6, based on quantitative amino acid analyses of a number of expressed forms of the *b* subunit.

2.5 Circular dichroism and differential scanning calorimetry.

Samples of b_{34-156}, or related chimeras purified as described above, were dialyzed into 20 mM sodium phosphate, pH 7.0, containing 100 mM NaCl. The same samples, but at different concentrations, were used for CD and DSC analyses. CD studies were carried out using a Jasco J-810 spectropolarimeter equipped with water-jacketed cells and a circulating bath. Spectra were recorded from 195-250 nm in 1-nm steps. Spectra were normalized to that of b_{34-156} using the isodichroic point of 203 nm for the helix-coil transition [26]. Temperature scans were collected at 222 nm for the range of 10 °C to 85 °C with 1 min equilibration times. Data were converted to mean residue ellipticity by standard methods. Thermal denaturation data were fitted to a two-state model [27, 28] as described [29]. Differential scanning calorimetry was carried out using a VP-DSC (MicroCal) differential scanning calorimeter, at rate of 1°C/min. Data were collected, and buffer-buffer reference scans subtracted, using Microcal software and the major transition fitted using Origin 5.

3. Results

3.1 Initial dimerization domain chimeras

The *b* subunit dimer of *E. coli* ATP synthase has been characterized as a highly helical four-domain protein (Fig. 1A), and the region responsible for dimerization, residues 53-122, as a novel, two-stranded right-handed coiled coil [13]. Before replacing parts of the coiled coil region with sequences that adopt different structures, we determined its tolerance for homologous sections of *b* subunits from two other organisms with homodimeric stator stalks. These initial chimeras were constructed in pDM8, which carries a synthetic sequence encoding the entire *b* subunit under control of *tac* promoter; the plasmid also carries the *lac* repressor. This plasmid can be used in conjunction with strain KM2 [21], which has a chromosomal deletion of *uncF*, encoding the *b* subunit, to test *b* subunit function.

Genomic DNA from *B. subtilis* and *T. maritima* was obtained and relevant sections of the *uncF* gene were amplified by PCR. Primers incorporated restriction sites to allow cloning of the PCR product into pDM8 [6] utilizing the BglII and BlpI sites, located in portions of the sequence encoding residues Lys-52—Leu54 and Ala-111—Arg-113, respectively. The relevant sections of the dimerization domains of parental *E. coli b* and the resulting chimeras, called Bs-1 and Tm-1, are shown in Fig. 1, with the foreign residues in color. Comparison of these three sequences reveals the conserved sequence characteristics of the 11-residue hendecad pattern, where the *a* and *h* positions are most often occupied by small residues, while the *d* and *e* positions are often occupied by larger nonpolar residues. These *a*, *d*, *e* and *h* positions define a hydrophobic strip with a right-handed slant, highlighted with pale green in the helical net diagrams shown for *E. coli* and Tm-1 in Fig. 2. Even though substantial differences can be seen between the sequences at most positions, the right-slanted hydrophobic strip is maintained in the Bs-1 and Tm-1 chimeras. Both of these chimeras supported normal growth of KM2 on the nonfermentable carbon sources acetate and succinate, indicating their capacity to function in ATP synthase in the process of oxidative phosphorylation. No IPTG was used in these tests, as previous studies have shown expression of *b* from pDM8 to be sufficiently leaky that induction is not necessary [23].

To evaluate the importance of the right-handed nature of the coiled coil, we also incorporated the well-characterized leucine zipper of yeast GCN4, a left-handed coiled coil of approximately 28 residues. Since the hydrophobic strip of a left-handed coiled-coil will have a left handed slant on the helical surface, replacement of a given number of residues of a RHCC with the same number of residues from a LHCC results in a discontinuity in the hydrophobic surface at one end of the foreign sequence, as seen in the diagram labeled "GCN4-1C" in Fig. 2. This discontinuity in the hydrophobic face would be expected to disrupt the helix-helix interaction. A continuous hydrophobic face can be maintained, however, by replacing 26 residues of the right-handed sequence with just 25 residues from a left-handed sequence, as seen for the GCN4-1 chimera sequence (see Figs. 1 and 2). Since it has been established that the *b* subunit tolerates lengthening or shortening by a number of residues [30-32], we viewed this one-residue reduction in length as unlikely to disrupt structure or function. The GCN4-1 chimera was constructed utilizing the AflII and BsiWI sites, encoding residues Leu-65—Lys-66 and Arg-98—Thr-99, respectively, but it failed to support more than a slight trace of growth on

nonfermentable carbon sources under any conditions of induction that were tested, even after three days incubation at 37 °C.

3.2 Characterization of membranes containing the Tm-1 and GCN4-1 chimeric b subunits.

Cells of strain KM2 carrying pDM8, or derivatives encoding the Tm-1 and GCN4-1 chimeras, were grown in LB media containing IPTG at a level that was previously shown to result in expression of b from pDM8 at level similar to that expressed from the normal chromosomal unc operon [6]. The ATP synthase content of membranes prepared from these cells was determined by western blotting using anti-α and anti-b antibodies, and by ATPase assays conducted under conditions where the F_1-ATPase dissociates from the membrane and expresses its full activity. As seen by the blot probed with the anti-α antibody (Fig. 3A), both the Tm-1 and GCN4-1 chimeras supported assembly of levels of ATP synthase similar to that observed with pDM8 ($uncF^+$ plasmid), while no more than a trace of α was bound to the membranes when no form of b was provided ($uncF$ plasmid). ATPase activity assays showed the membranes from strain 1100, the parent of KM2, to contain the highest levels of ATPase (0.46 U/mg), followed by those with pDM8 (0.33 U/mg) and the Tm-1 chimera (0.34 U/mg), while those with the GCN4-1 chimera were again somewhat lower (0.27 U/mg). Cells lacking any form of b had just 0.03 U/mg of ATPase activity. A polyclonal antibody raised to $E.\ coli\ b$ subunit recognized all of the chimeric b subunits (Fig. 3A). These results show that assembly of ATP synthase was not significantly affected by the Tm-1 chimera, but was modestly reduced by the GCN4-1 chimera.

ATP-dependent proton pumping by the membrane vesicles was determined using the ACMA fluorescence quenching assay (Fig. 3B). In general, levels of quenching were consistent with the measured ATPase content. Membranes with the Tm-1 chimera repeatedly showed higher levels of quenching in comparison to those with pDM8, suggesting a tighter coupling. Membranes carrying enzyme with the GCN4-1 chimera showed somewhat lower proton pumping. While this may reflect in part the lowered assembly, the magnitude of the decline suggests that the enzyme was partially uncoupled. Overall, however, given the failure of the GCN4-1 chimera to support significant growth on nonfermentable carbon sources, the levels of ATP synthase assembly and ATP-dependent proton pumping were surprising.

3.3 Chimeras containing larger segments of T. maritima sequence and the effect of induction levels on complementation using different expression plasmids

Given the complementation by the initial dimerization domain chimeras incorporating other eubacterial b sequences, we explored the possibility that $E.\ coli$ ATP synthase might accommodate larger segments of $T.\ maritima\ b$ sequence. Among the forms prepared were chimeras in which the foreign sequence extended part or all of the way to the termini of the polypeptide. The chimeras were tested for support of growth on acetate media at several IPTG concentrations in case higher-level expression was necessary (Table 1). In the absence of IPTG, growth was also supported by chimera Tm-2, in which the foreign sequence was extended to residue 124 of $E.\ coli$, and traces of growth were seen with chimeras in which the Thermotoga

8

sequence began at position 37. Surprisingly, induction of the chimeras by as little as 3 µM IPTG resulted in poorer growth; even with pDM8, growth was severely inhibited at 10 µM IPTG.

While the mechanism of growth inhibition by higher levels of expression of *b* or *b* chimeras has yet to be established, this finding raised concerns that the pDM8 system, which uses the inherently leaky *tac* promoter from pKK223-3 [33], might give false negative results due to excessive expression. Leakiness would be amplified by growth on acetate since it is not a preferred carbon source. We therefore transferred the *E. coli uncF* sequence from pDM8 into pBAD24 [22], which provides more stringent repression in the absence of the inducer arabinose, producing plasmid pSD205. Concentrations of 0, 3, 10, and 30 µM arabinose were then used to induce expression. pSD205 supported only a trace of growth by KM2 on acetate with no inducer present, modest colonies (+) at 3 µM arabinose, moderate colonies (++/+++) at 10 µM, and full growth, equivalent to that of the positive control strain 1100/pSD80, (+++) at 30 µM arabinose. Similar results were observed with pSD248, which contains the Tm-1 chimera in pBAD24, although growth was slightly less than for pSD205 except at 30 µM arabinose, where it was equivalent. No growth was seen, even at 30 µM arabinose, for KM2/pSD80, the *uncF* control, indicating that the inducer did not serve as a significant carbon source, at least up to this concentration. These results implied that reliable determinations of complementation could be made using this system. Subsequent complementation studies employed the pBAD24 system, using 0, 10 and 30 µM arabinose as inducer.

3.4 Complementation of KM2 by additional chimeric b subunits expressed from pBAD constructs

Most of the previously described chimeras were transferred to pBAD24, and additional ones from a number of exogenous sources were constructed for testing complementation in strain KM2. We began with a re-examination of the extent of *T. maritima b* sequence that could be incorporated with retention of function, then extended the analysis to chimeras that incorporated sequences from less closely related proteins having the hendecad repeat pattern of *b*, and finally to a number of chimeras that incorporated either the GCN4 leucine zipper, or else other left handed coiled coils. Chimeras were designed to conserve the hendecad reading frame when possible, or to maintain a continuous hydrophobic surface on the helix, except for some of those incorporating left-handed coiled coils. Here, in addition to those chimeras designed as outlined in Fig. 2, we also constructed several control chimeras, given designations terminating with "C", in which equal numbers of residues were removed and inserted. In no case did stronger induction of a chimera result in poorer growth. Similar relative rates of growth were obtained on succinate as on acetate, although growth on succinate was faster.   The various plasmids expressing chimeric forms of *b* and the strength of growth they supported at 30 µM arabinose are summarized in Table 2. Membranes were also prepared from cells expressing a number of these chimeras for determination of their ATP synthase content and ATP-dependent proton-pumping activities (Fig. 4).

Results presented in Table 2 confirmed the abilities of chimeras with *T. maritima* sequence extending from positions 37-124 to support oxidative phosphorylation, although

9

growth was not so rapid as with Tm-1. Extension of the exogenous sequence C-terminally to position 124 was more detrimental than extension N-terminally to position 37. Analysis of membranes for ATPase activity (see legend for Fig. 4)) showed that these additional exogenous residues, particularly in positions 109-124, significantly reduced assembly, and the lower levels were reflected in decreased proton pumping (Fig. 4 *upper set*). It is notable, however, that even though membranes with chimeras Tm-1 and Tm-7 contained somewhat lower levels of ATPase activity than those from the normal *E. coli* sequence, their proton pumping was at least as strong. Thus these enzymes are fully coupled.

The E subunit from the bacterial V-type ATPase of *Chlamydia pneumoniae* contains a section near the N terminus bearing a strong hendecad repeat pattern with position occupancy similar to that seen in bacterial *b* subunits, but also with some interesting differences, including a proline at position 24, near the beginning of the hendecad pattern. Chimera VATE-8, in which 38 residues (Glu-26—His-63) from the E subunit were inserted in place of the normal residues Lys-58—Glu-95, showed full growth.   Extending the foreign sequence just three residues toward the N-terminus, which included Pro-24, however, strongly reduced growth (see VATE-2). In addition, when sequences from the E subunit were inserted into *E. coli* positions 96-110 (VATE-4, -5, or –6) only faint growth was observed. Analysis of membranes showed VATE-2 to support assembly of ATP synthase well (see legend to Fig. 4), but a lower level of assembly seen for VATE-7 in this set was accompanied by a higher level of proton pumping (Fig. 4 *middle set*), suggesting a partial uncoupling produced by the proline residue in VATE-2. All of the chimeras that were analyzed in which the VATE sequence extended to position 110 showed substantially reduced assembly and modest ATP-dependent proton pumping, as seen here for VATE-5.

Ag84 is a minor antigen produced by *M. tuberculosis* [20]. The sequence of the protein indicates it to be a member of the DivIVA family believed to function as a marker for the cell poles during cell division in gram positive bacteria [34]. Our examination of the sequence of this class of protein showed it to have an extended region of hendecad repeat similar to the pattern in the dimerization domain of *b*. Ag84 was therefore a source of foreign sequence, unrelated to either F-ATP synthase or V-ATPases, that might provide for functional *b* chimeras. In the Ag84-1 chimera, residues Asp-55 to Glu-110 of *E. coli b*, the same residues that had been replaced successfully by the corresponding sequences from *B. subtilis* and *T. maritima*, were substituted by a segment of the Ag84 hendecad sequence, to produce the Ag84-1 chimera, which failed to complement KM2 (Table 2). Restoring the *E. coli b* residues to positions 96-110 in chimera Ag84-2 restored normal growth on acetate, while restoration of the normal residues to positions Asp-55—Glu-71 in Ag84-3 had no effect. Analysis of membrane vesicles prepared from these strains showed moderately reduced assembly and proton pumping (Fig. 4 legend, and lower set) for chimeras VATE-1 and VATE-3, again implying the importance of positions in the 96-110 region.

The GCN4-1 chimera was transferred into the pBAD vector, and a number of additional chimeras were constructed. These incorporated the left-handed coiled coil in a number of

different frames and positions (Table 2), either with or without the one-residue deletion necessary for maintaining the hydrophobic face. In addition, left-handed coiled coils from rabbit tropomyosin and human Eea1, an endosome associated protein, were used to ensure that the failure to obtain complementing chimeras was a general property of left-handed coiled coils, rather than specific to GCN4. Under no circumstances was more than a faint trace of growth evident. Levels of ATPase activity in membranes prepared from KM2 containing these chimeras were variable but usually low. In cases where significant ATPase was found in the membranes, significant proton pumping was observed (data not shown), in agreement with the results shown for GCN4-1 in Fig. 3.

3.5 Denaturation analysis of soluble forms of chimeric b subunits

To study the effects of the exogenous sequences on the conformation and stability of b, chimeras Tm-1, Ag84-1, and GCN4-1 were expressed in the soluble form, b_{34-156}. The proteins were purified and their CD spectra were collected at 10 °C for comparison to that of normal b_{34-156} (Fig. 5a). All of the spectra indicated predominantly helical structure. Tm-1 gave the strongest signal at 222 nm, with θ_{222}=-40,000, indicative of essentially 100% helical structure. The spectrum of the GCN4-1 chimera was virtually identical to that of b_{34-156}, while the spectrum of Ag84-1 indicated the lowest helicity.

Thermal denaturation in the CD revealed very significant differences between the constructs, however (Fig. 5b). The normal *E. coli* b_{34-156} exhibited a cooperative transition with melting midpoint of 37 °C, consistent with earlier determinations [7]. For the Tm-1 chimera, the major transition occurred in a highly cooperative manner with a midpoint of 61 °C. In contrast, the Ag84-1 chimera melted with a cooperativity similar to that of the wild-type sequence, but at a substantially lower temperature. Since the protein was partially unfolded at 10 °C, the midpoint was not well-defined but would appear to be in the range of 25 °C. The melting transition of the GCN4-1was much broader, indicating a lowered cooperativity. Despite this, the midpoint of 62 °C was similar to that of Tm-1.

Denaturation of these constructs was also followed by differential scanning calorimetry, using protein concentrations 2- to 3-fold higher than those used in the CD analysis to obtain better-defined signals (Fig. 6). Again, the similarity of the transitions of b_{34-156} and the Tm-1 and Ag84-1 chimeras was notable, aside from the major differences in the midpoint values of the transitions, 40 °C, 67 °C, and 29 °C, respectively. Differences in these values from those of the CD analyses are expected due to the monomer-dimer nature of the system and the different concentrations used. The GCN4-1 chimera melted over a broad temperature range and was not modeled well as a single transition; the peak of heat absorption was at 69 °C.

4. Discussion

4.1 Tolerance of the coiled coil domain for substitution by different sequences

Not surprisingly, we found that *E. coli* b tolerated the largest exogenous sequences from orthologous b subunits, with most of the dimerization domain being substituted without deleterious effects despite the substantial sequence differences. Based on mapping of the b_2-F_1 interaction by cross-linking/mass spectometry [35], much of the dimerization domain region is

located between F_0 and the lower surface of F_1, where no contact is made with other subunits. It is likely that the impaired growth seen when more N- or C-terminal regions were included resulted from impaired interactions with the *a* subunit and with $\alpha_3\beta_3$, respectively. Generally similar results were recently reported using the *b* and *b'* subunits from *Thermosynechococcus elongatus* [36]. Other sequences with the characteristic hendecad pattern, even the unrelated DivIVA protein Ag84, substituted functionally into the region between positions 55-95, but could not be extended toward the C terminus. The region containing positions 55-95 is essentially the section in which a close relationship of neighboring *a* and *h* positions between the two subunits has been established [13]. Changes in the pattern of position occupancy C-terminal to this region suggest an altered relationship between the helices [11].

In contrast we found no *in vivo* oxidative phosphorylation by any of the left-handed coiled coil chimeras, despite the different sequences used, the different insertion sites, and maintenance of the hydrophobic surface that we expected to favor accommodation of foreign sequence. These results strongly suggest that the stator stalk does not adopt a classical left-handed coiled coil structure, which would accommodate such a substitution. In light of the assembly of ATP synthase containing the GCN4-1 chimera, the present results also suggest that a left-handed coiled coil structure may be inconsistent with stator stalk function. Overall, the properties of the GCN4-1 chimera are similar to those of uncoupled, single-residue deletion mutants in the 100-105 region [23].

The different effects of chimeras on the two functional assays we used, growth on nonfermentable carbon sources and ATP-dependent proton pumping in membrane vesicles, is notable. While these two activities require the enzyme to function in opposite directions, the difference could also result from the required strength of protonmotive force. In the proton pumping assay, generation of a modest protonmotive force is readily detectable, whereas growth on nonfermentable carbon sources is likely to require a very substantial protonmotive force, and a b_2 structure that can resist a strong torque imparted by proton-driven rotation of $\gamma\epsilon c_{10}$ [13, 37].

4.2 Relationship of functionality to structure and stability of soluble forms of the chimeras.

The similarities of the CD spectra of the Tm-1, GCN4-1, and Ag84-1 chimeras imply that the exogenous sequences did not cause gross structural differences compared to the parental $b_{34\text{-}156}$, *i.e.* all retained their overall helical, coiled coil nature. *T. maritima* is a hyperthermophile [38], so thermostability of Tm-1 was not unexpected. The isolated GCN4 leucine zipper is also relatively thermostable with a T_m of 64 °C [39]. Since both chimeric constructs showed elevated thermal stability, and Tm-1 supported oxidative phosphorylation, the nonfunctionality of the GCN4-1 construct cannot be attributed to this feature. The *T. maritima b* sequence was expected to fit well into the *E. coli* subunit, and the high cooperativity of unfolding of the Tm-1 chimera confirms this to be the case. In contrast, the low cooperativity of melting of the GCN4-1 chimera implies that the exogenous sequence did not stabilize the structure of the residual *b* residues. This effect can be explained by a discontinuity between the in-register nature of the helices in the two stranded left-handed coiled coil of GCN4, with knobs-into-holes packing of side chains at the interface [40], and the offset helices we proposed for the right-handed coiled

coil of b_2 [10, 13]. We expect the greater stability of the left-handed coiled coil to dominate the chimera, requiring that the residual b sequence also adopt an in-register alignment. This conformation would be stabilized relative to the unfolded state to some degree by the hydrophobic nature of the surfaces, but any particular favorable interactions characteristic of the offset orientation would be lost, resulting in the non-cooperative melting seen in Figs. 5B and 6D.

Nevertheless, given the higher overall stability of the GCN4-1 chimera, why did it fail to support oxidative phosphorylation? If b function requires significant movement of the b helices relative to one another, the knobs-into-holes packing should restrict that, but substantial ATP dependent proton pumping was still observed. The offset alignment provides stronger interactions with F_1 [10], and this could be a factor. Alternatively, the particular favorable interactions characteristic of the right-handed, offset orientation may be essential to resisting the torque at high protonmotive forces.

We were surprised by the low stability, but cooperative unfolding, of the Ag84-1 chimera. While little is known about the nature of the coiled coil region of this protein [34], the hendecad pattern is clear from the sequence. Since this protein is evolutionarily unrelated to the b subunit, its function may not require stabilizing interactions present in b. Additional studies with functional chimeras would be required to determine the relationship between lowered thermodynamic stability and b functionality. It remains notable, however, that at least 37 residues of b could be replaced by a sequence from Ag84, with no evident loss of functionality.

Acknowledgements

References

[1]   A.E. Senior, S. Nadanaciva, J. Weber, The molecular mechanism of ATP synthesis by F_1F_0-ATP synthase, Biochim. Biophys. Acta 1553 (2002) 188-211.

[2]   M. Nakanishi-Matsui, M. Futai, Stochastic proton pumping ATPases: from single molecules to diverse physiological roles, IUBMB Life 58 (2006) 318-322.

[3]   T.M. Duncan, The ATP Synthase: Parts and Properties of a Rotary Motor, in: D.D. Hackney, F. Tamanoi (Eds.), The Enzymes: Energy Coupling and Molecular Motors vol. 23, Elsevier Academic Press, New York, 2004, pp. 203-275.

[4]   S. Wilkens, Rotary molecular motors, Adv. Protein Chem. 71 (2005) 345-382.

[5]   S.D. Dunn, The polar domain of the b subunit of *Escherichia coli* F_1F_0-ATPase forms an elongated dimer that interacts with the F_1 sector, J. Biol. Chem. 267 (1992) 7630-7636.

[6] D.T. McLachlin, S.D. Dunn, Dimerization interactions of the *b* subunit of the *Escherichia coli* F_1F_0-ATPase, J. Biol. Chem. 272 (1997) 21233-21239.

[7] M. Revington, S.D. Dunn, G.S. Shaw, Folding and stability of the *b* subunit of the F_1F_0 ATP synthase, Protein Sci. 11 (2002) 1227-1238.

[8] M. Revington, D.T. McLachlin, G.S. Shaw, S.D. Dunn, The dimerization domain of the *b* subunit of the *Escherichia coli* F_1F_0-ATPase, J. Biol. Chem. 274 (1999) 31094-31101.

[9] D.T. McLachlin, J.A. Bestard, S.D. Dunn, The *b* and δ subunits of the *Escherichia coli* ATP synthase interact via residues in their C-terminal regions, J. Biol. Chem. 273 (1998) 15162-15168.

[10] K.S. Wood, S.D. Dunn, Role of the asymmetry of the homodimeric b_2 stator stalk in the interaction with the F_1 sector of *Escherichia coli* ATP synthase, J. Biol. Chem. 282 (2007) 31920-31927.

[11] S.D. Dunn, D.J. Cipriano, P.A. Del Rizzo, ATP Synthase stalk subunits *b*, δ, and ε: structures and functions in energy coupling, in: M. Futai, Y. Wada (Eds.), Handbook of ATPases, Springer-Verlag, Weinheim, 2004, pp. 311-338.

[12] P.A. Del Rizzo, Y. Bi, S.D. Dunn, B.H. Shilton, The "second stalk" of *Escherichia coli* ATP synthase: structure of the isolated dimerization domain, Biochemistry 41 (2002) 6875-6884.

[13] P.A. Del Rizzo, Y. Bi, S.D. Dunn, ATP synthase *b* subunit dimerization domain: a right-handed coiled coil with offset helices, J. Mol. Biol. 364 (2006) 735-746.

[14] A. Lupas, Coiled coils: new structures and new functions, Trends Biochem. Sci. 21 (1996) 375-382.

[15] A.N. Lupas, M. Gruber, The structure of α-helical coiled coils, Adv. Protein Chem. 70 (2005) 37-78.

[16] T. Hornung, O.A. Volkov, T.M.A. Zaida, S. Delannoy, J.G. Wise, P.D. Vogel, Structure of the cytosolic part of the subunit *b*-dimer of *Escherichia coli* F_0F_1-ATP synthase, Biophys. J. (2008) *in press.*

[17] J.G. Wise, P.D. Vogel, Subunit *b* dimer of the *Escherichia coli* ATPase can form left-handed coiled coils, Biophys. J. (2008) *in press.*

[18] K.A. McCormick, B.D. Cain, Targeted mutagenesis of the *b* subunit of F_1F_0 ATP synthase in *Escherichia coli*: Glu-77 through Gln-85, J. Bacteriol. 173 (1991) 7240-7248.

[19] A.C. Porter, C. Kumamoto, K. Aldape, R.D. Simoni, Role of the *b* subunit of the *Escherichia coli* proton-translocating ATPase. A mutagenic analysis, J. Biol. Chem. 260 (1985) 8182-8187.

[20] P.W. Hermans, F. Abebe, V.I. Kuteyi, A.H. Kolk, J.E. Thole, M. Harboe, Molecular and immunological characterization of the highly conserved antigen 84 from *Mycobacterium tuberculosis* and *Mycobacterium leprae*, Infect. Immun. 63 (1995) 954-960.

[21] K.A. McCormick, G. Deckers-Hebestreit, K. Altendorf, B.D. Cain, Characterization of mutations in the *b* subunit of F_1F_0 ATP synthase in *Escherichia coli*, J. Biol. Chem. 268 (1993) 24683-24691.

[22] L.M. Guzman, D. Belin, M.J. Carson, J. Beckwith, Tight regulation, modulation, and high-level expression by vectors containing the arabinose PBAD promoter, J. Bacteriol. 177 (1995) 4121-4130.

[23] D.J. Cipriano, K.S. Wood, Y. Bi, S.D. Dunn, Mutations in the dimerization domain of the *b* subunit from the *Escherichia coli* ATP synthase. Deletions disrupt function but not enzyme assembly, J. Biol. Chem. 281 (2006) 12408-12413.

[24] D.J. Cipriano, Y. Bi, S.D. Dunn, Genetic fusions of globular proteins to the ε subunit of the *Escherichia coli* ATP synthase: Implications for *in vivo* rotational catalysis and ε subunit function, J. Biol. Chem. 277 (2002) 16782-16790.

[25] M.M. Bradford, A rapid and sensitive method for the quantitation of microgram quantities of protein utilizing the principle of protein-dye binding, Anal. Biochem. 72 (1976) 248-254.

[26] M.E. Holtzer, A. Holtzer, α-helix to random coil transitions: determination of peptide concentration from the CD at the isodichroic point, Biopolymers 32 (1992) 1675-1677.

[27] M.M. Santoro, D.W. Bolen, Unfolding free energy changes determined by the linear extrapolation method. 1. Unfolding of phenylmethanesulfonyl α-chymotrypsin using different denaturants, Biochemistry 27 (1988) 8063-8068.

[28] L. Swint, A.D. Robertson, Thermodynamics of unfolding for turkey ovomucoid third domain: thermal and chemical denaturation, Protein Sci. 2 (1993) 2037-2049.

[29] L.-A.K. Briere, S.D. Dunn, The Periplasmic Domains of *Escherichia coli* HflKC Oligomerize through Right-Handed Coiled-Coil Interactions, Biochemistry 45 (2006) 8607-8616.

[30] D. Bhatt, S.P. Cole, T.B. Grabar, S.B. Claggett, B.D. Cain, Manipulating the length of the *b* subunit F_1 binding domain in F_1F_0 ATP synthase from *Escherichia coli*, J. Bioenerg. Biomembr. 37 (2005) 67-74.

[31] P.L. Sorgen, M.R. Bubb, B.D. Cain, Lengthening the second stalk of F_1F_0 ATP synthase in *Escherichia coli*, J. Biol. Chem. 274 (1999) 36261-36266.

[32] P.L. Sorgen, T.L. Caviston, R.C. Perry, B.D. Cain, Deletions in the second stalk of F_1F_0-ATP synthase in *Escherichia coli*, J. Biol. Chem. 273 (1998) 27873-27878.

[33] J. Brosius, A. Holy, Regulation of ribosomal RNA promoters with a synthetic *lac* operator, Proc. Natl. Acad. Sci. U S A 81 (1984) 6929-6933.

[34] L. Nguyen, N. Scherr, J. Gatfield, A. Walburger, J. Pieters, C.J. Thompson, Antigen 84, an effector of pleiomorphism in *Mycobacterium smegmatis*, J. Bacteriol. 189 (2007) 7896-7910.

[35] D.T. McLachlin, A.M. Coveny, S.M. Clark, S.D. Dunn, Site-directed cross-linking of *b* to the α, β, and *a* subunits of the *Escherichia coli* ATP synthase, J. Biol. Chem. 275 (2000) 17571-17577.

[36] S.B. Claggett, T.B. Grabar, S.D. Dunn, B.D. Cain, Functional incorporation of chimeric *b* subunits into F_1F_o ATP synthase, J. Bacteriol. 189 (2007) 5463-5471.

[37] D.A. Cherepanov, A.Y. Mulkidjanian, W. Junge, Transient accumulation of elastic energy in proton translocating ATP synthase, FEBS Lett. 449 (1999) 1-6.

[38] K.O. Stetter, History of discovery of the first hyperthermophiles, Extremophiles 10 (2006) 357-362.

[39] A.I. Dragan, P.L. Privalov, Unfolding of a leucine zipper is not a simple two-state transition, J. Mol. Biol. 321 (2002) 891-908.

[40] E.K. O'Shea, J.D. Klemm, P.S. Kim, T. Alber, X-ray structure of the GCN4 leucine zipper, a two-stranded, parallel coiled coil, Science 254 (1991) 539-544.

Table 1.

Strain/plasmid/*b* type	Exogenous residues inserted[a]	*E. coli* residues replaced	Growth on acetate[b] [IPTG] (μM)				
			0	1	3	10	30
1100/pSD80/WT	na[c]	na	+++	+++	+++	+++	+++
KM2/pSD80/none[d]	na	na	-	-	-	-	-
KM2/pDM8/WT[d]	none	none	+++	+++	++	+	tr[e]
KM2/pSD200/Tm-1	E58-Q111	D55-E108	+++	++	+	-	-
KM2/pSD246/Tm-2	E58-A127	D55-V124	++	++	tr	-	-
KM2/pJW3/Tm-3	M1-Ser164	M1-L156	-	-	-	-	-
KM2/pJW4/Tm-4	R40-Ser164	Q37-L156	-	-	-	-	-
KM2/pJW5/Tm-5	M1-Ala127	M1-V124	-	-	-	-	-
KM2/pJW6/Tm-6	R40-Ala127	Q37-V124	tr	-	-	-	-
KM2/pSD245/Tm-7	R40-Q111	Q37-E108	tr	tr	-	-	-
KM2/pPK2/Bs-1	Q65-V120	D55-E110	+++	+++	+	-	-
KM2/pSD203/GCN4-1	Q252-V278	K67-A94	tr	tr	-	-	-

[a]Inserted sequences are from *T. maritima* except for pPK2 which was from *B. subtilis*. [b]Growth was tested on minimal medium with 0.2 % sodium acetate as described under Experimental Procedures. Growth was scored based on colony diameter after incubation at 37 °C for 2 days as follows: +++, >0.4 mm; ++, 0.25-0.4 mm; +, 0.1-0.25 mm; tr, <0.1 mm. All strains grew well on glucose.
[c]na, not applicable.
[d]pSD80 is the negative control plasmid while pDM8 is the positive control with *E. coli b* sequence.
[e]tr, trace.
Complementation of *uncF* strain KM2 by chimeric *b* subunits

Table 2
Growth on acetate medium of KM2 with *b* subunit chimeras in pBAD24

Sequence source	Designation	Exogenous residues inserted	*E. coli* residues replaced	Plasmid	Growth[a]
E. coli b subunit					
	WT	none	none	pSD205	+++
	null	na[b]	na[b]	pBAD24	-
T. maritima b subunit					
	Tm-1	E58-Q111	D55-E108	pSD248	+++
	Tm-2	E58-A127	D55-V124	pSD252	+
	Tm-6	R40-A127	Q37-V124	pSD247	+
	Tm-7	R40-Q111	Q37-E108	pSD251	++
C. pneumoniae V-ATPase E subunit					
	VATE-1	K23-K78	D55-E110	pSD250	-
	VATE-2	K23-H63	D55-E95	pSD255	+
	VATE-3	E26-K78	K58-E110	pSD256	+
	VATE-4	N35-K78	K67-E110	pSD257	+
	VATE-5	E26-K67	K69-E110	pSD258	-
	VATE-6	E26-K78	K58-E110	pSD259	-
	VATE-7	N35-H63	K67-E95	pSD260	+++
	VATE-8	E26-H63	K58-E95	pSD264	+++
M. tuberculosis Ag84					
	Ag84-1	S108-A163	D55-E110	pSD204	-
	Ag84-2	S108-D148	D55-E95	pSD277	+++
	Ag84-3	S125-A163	A72-E110	pSD278	-
	Ag84-4	S125-D148	A72-E95	pSD279	+++
Left-handed coiled coils					
	GCN4-1	Q252-V278	K67-A94	pSD249	tr[c]
	GCN4-1C[d]	Q252-V278	A68-A94	pSD280	-
	GCN4-2	Q252-V278	E71-R98	pSD253	-
	GCN4-2C	Q252-V278	A72-R98	pSD254	-
	GCN4-4	V257-K275	A61-N80	pSD261	tr
	GCN4-5	V257-K275	A72-K91	pSD262	tr
	GCN4-5C	V257-K275	Q73-K91	pSD275	tr
	GCN4-7	V257-K275	R83-V102	pSD270	-
	GCN4-8	V257-K275	A61-N80, R83A[e]	pSD271	tr
	GCN4-8C	V257-K275	T62-N80, R83A	pSD276	tr
	Eea1-1[f]	L1320-Q1338	A72-K91	pSD272	-
	Tropo-1[g]	V246-K264	A72-K91	pSD273	-

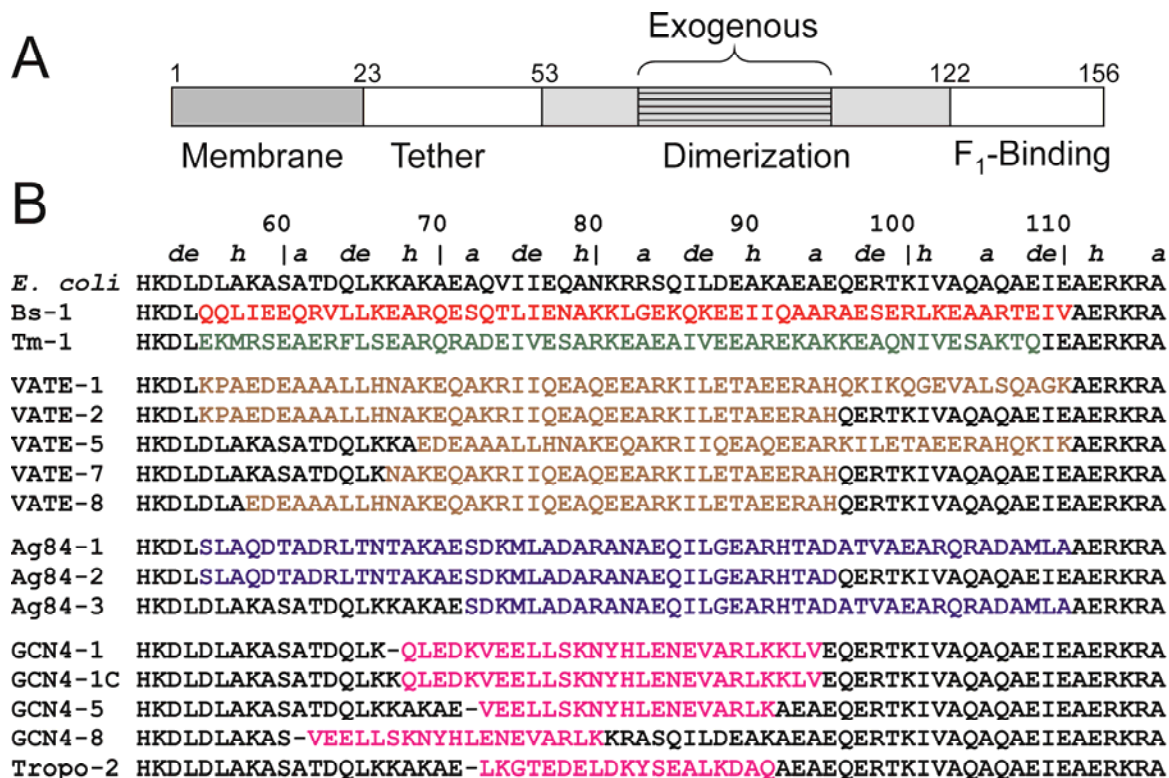|				
Tropo-2	L50-Q68	A72-K91	pSD274	-

Fig. 1. The *b* subunit of *E. coli* ATP synthase and a sampler of dimerization domain chimeras. (A) The domain structure of the 156-residue *b* subunit is shown. Most chimeras were prepared by replacement of residues within the dimerization domain with sequences from exogenous sources. (B) The sequences of a number of the dimerization domain chimeras that were produced and studied is presented. Numbering is according to the *E. coli* sequence; core hendecad positions are indicated. For each chimera shown, the exogenous sequence is in color. Exogenous sequences shown were derived from the *B. subtilis* (Bs-1) or *T. maritima* (Tm-1) *b* subunit, the E subunit of the V-type enzyme encoded by *C. pneumoniae* (VATE series), antigen-84 of *M. tuberculosis* (Ag84 series), or left-handed coiled coils of yeast transcription factor GCN4 or rabbit tropomyosin (Tropo-2).
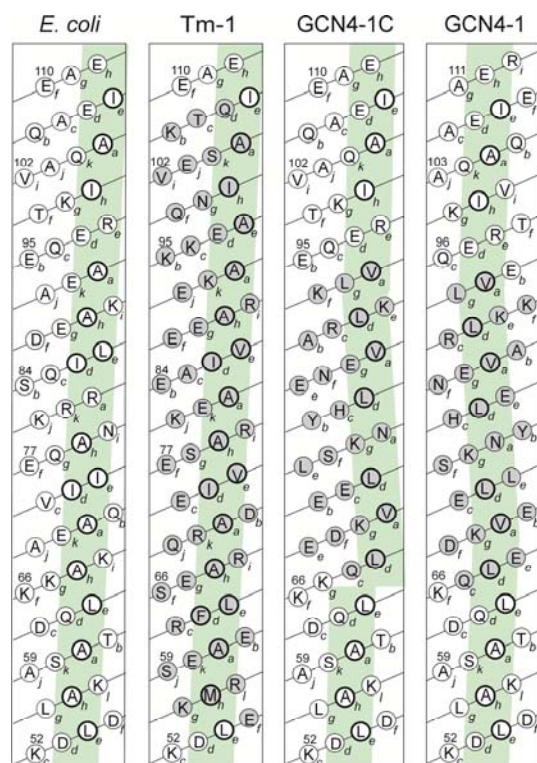
Fig. 2. Helical net diagrams of the *E. coli b* dimerization domain and selected chimeras. For each position, the residue and hendecad or heptad position are indicated. Normal *E. coli* residues are in white circles; exogenous residues are in gray circles. The broad green strips highlight the helical interfaces containing the *a*, *d*, *e* and *h* positions of hendecad patterns or the *a* and *d* positions of heptad patterns. Nonpolar residues in these strips are emphasized by bold circles.
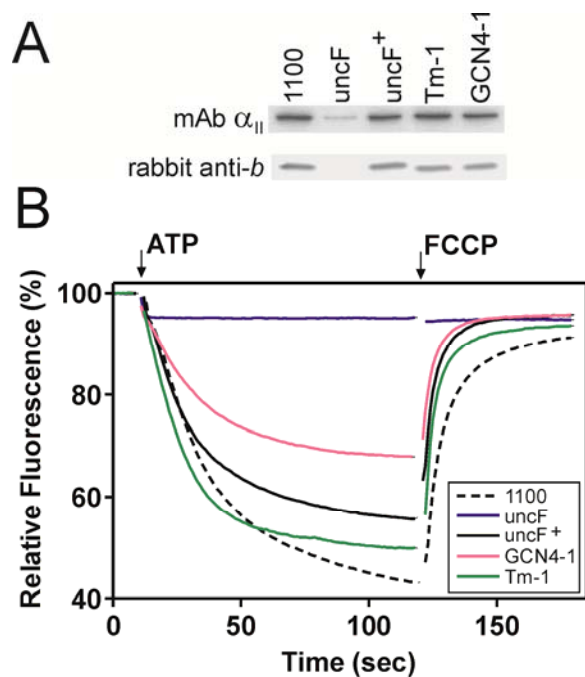
Fig. 3. Characterization of membrane vesicles carrying Tm-1 and GCN4-1 chimeras. Membranes were prepared from strains carrying plasmids as indicated: 1100, 1100 (wild-type)/pSD80(empty expression vector); uncF, KM2/pSD80; uncF$^+$, KM2/pDM8 (synthetic gene encoding b); Tm-1, KM2/pSD200; GCN4-1, KM2/pSD203. (A) The ATP synthase content of membrane preparations was compared by western blotting using ^{125}I-labelled antibodies to either the α subunit of F$_1$ (monoclonal antibody α_{II}) or to the b subunit of F$_0$ (polyclonal rabbit anti-b). (B) ATP-Dependent proton pumping was measured by quenching of fluorescence of ACMA. At the indicated times ATP and FCCP were added to concentrations of 2 mM and 2 μM, respectfully.
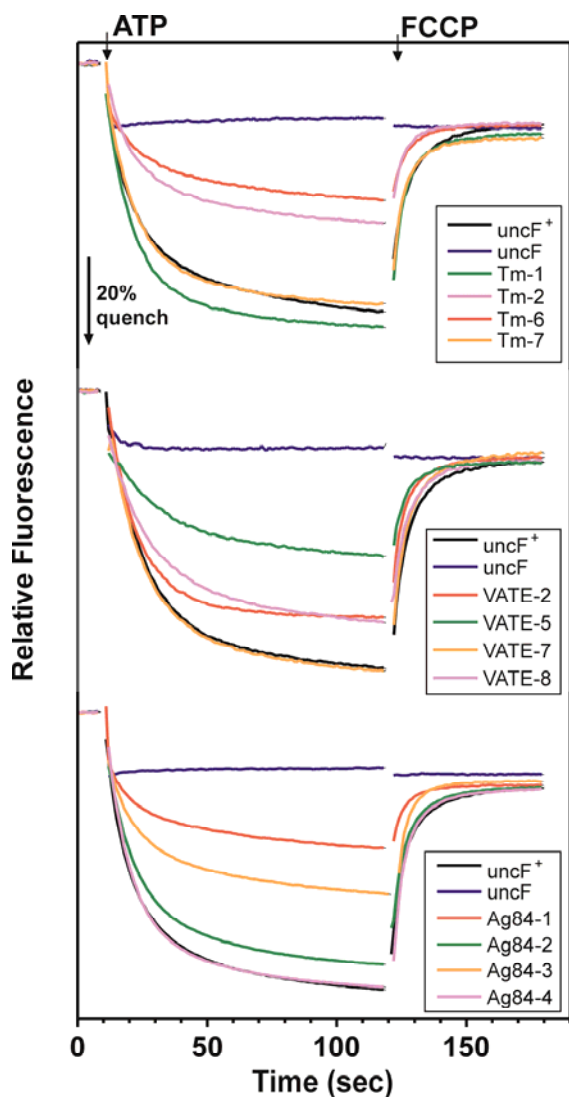
21

Fig. 4. ATP-Dependent proton pumping by membrane vesicles prepared from transformants of KM2 carrying chimeric *b* subunits. Membrane vesicles were prepared from cells of strain KM2 carrying plasmids based on pBAD24 that expressed the indicated *b* subunit chimeras as described in section 2.3. Details of the chimeras are provided in Table 2 and the sequences of the chimeras are shown in Fig. 1 (B). Membranes were analyzed for ATPase content and for ATP-dependent proton pumping. Upper set, membrane vesicles from cells carrying plasmids encoding *T. maritima b* subunit chimeras (chimera, plasmid, ATPase activity): uncF$^+$, pSD205, 0.46 U/mg; uncF, pBAD24, 0.06 U/mg; Tm-1, pSD248, 0.33 U/mg; Tm-2, pSD252, 0.19 U/mg; Tm-6, pSD247, 0.12 U/mg; Tm-7, pSD251, 0.29 U/mg. Middle set, membrane vesicles from cells carrying plasmids encoding *C. pneumoniae* E subunit chimeras: uncF$^+$, pSD205, 0.46 U/mg; uncF, pBAD24, 0.06 U/mg; VATE-2, pSD255, 0.33 U/mg; VATE-5, pSD258, 0.18 U/mg; VATE-7, pSD260, 0.25 U/mg; VATE-8, pSD264, 0.14 U/mg. Lower set, membrane vesicles from cells carrying plasmids encoding *M. tuberculosis* Ag84 chimeras: uncF$^+$, pSD205, 0.72 U/mg; uncF, pBAD24, 0.06 U/mg; Ag84-1, pSD204, 0.33 U/mg; Ag84-2, pSD277, 0.48 U/mg; Ag84-3, pSD278, 0.46 U/mg; Ag84-4, pSD279, 0.61 U/mg.
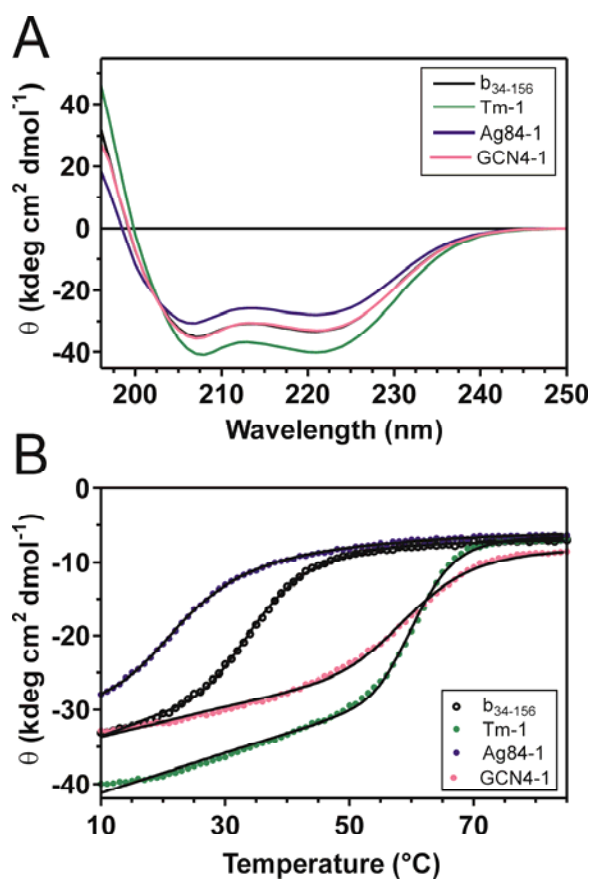
Fig. 5. Circular dichroism analysis of soluble forms of *b* chimeras. CD spectra (A) and thermal denaturation curves (B) of b_{34-156} and chimeric versions were collected and analyzed as described in section 2.5, using a buffer containing 20 mM sodium phosphate, pH, 7.0 and 100 mM NaCl. Samples were studied at a corrected concentration of 0.3 mg/ml, using a cell with a light path of 1 mm. The lines in (B) represent the best fit to a two-state denaturation model.
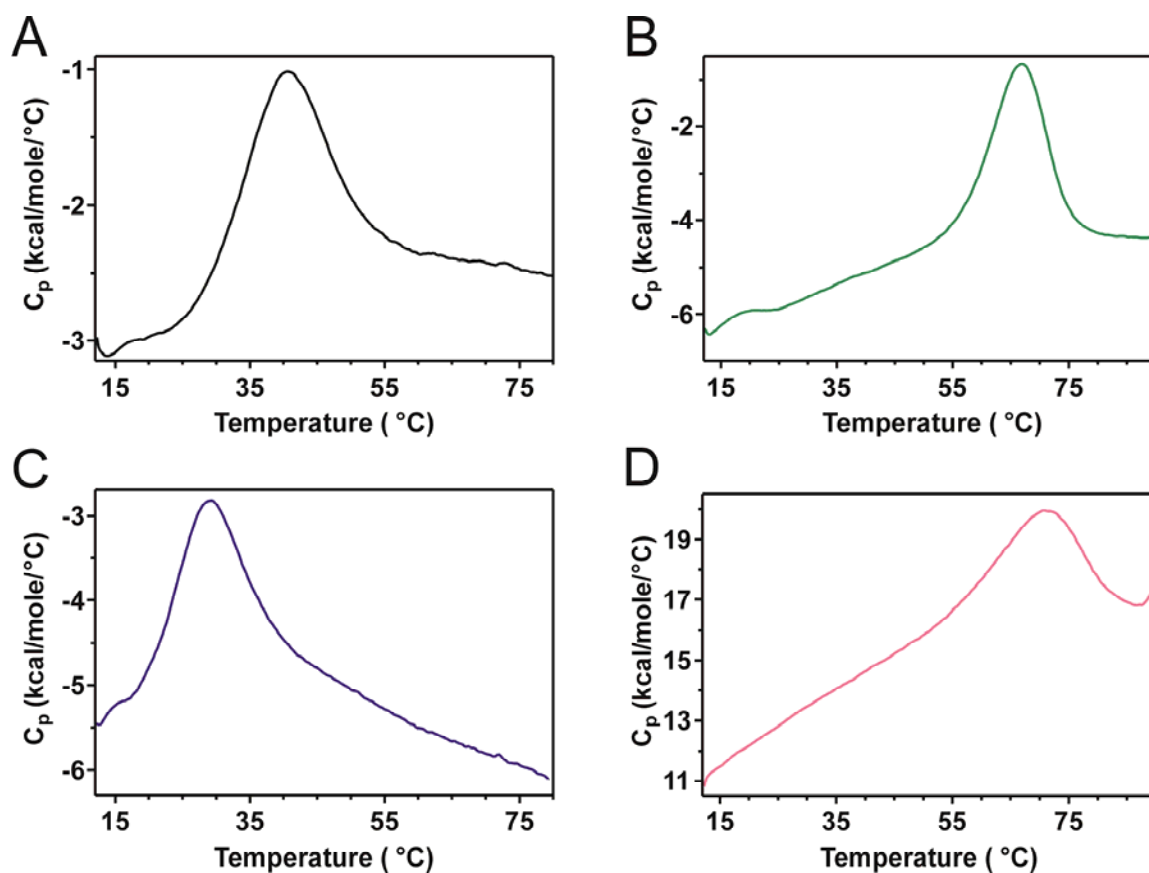
Fig. 6. Denaturation of soluble forms of *b* chimeras by differential scanning calorimetry. Samples were analyzed in 20 mM sodium phosphate buffer, pH, 7.0, containing 100 mM NaCl using a Microcal VP-DSC as described in section 2.5. Buffer-corrected thermograms are shown. Corrected concentrations, in mg/mL, for data presented were: (A) b_{34-156}, 0.80; (B) Tm-1, 0.60; (C) Ag84-1, 0.60; (D) GCN4-1, 0.66.